HHS Public Access

Author manuscript

J Leukoc Biol. Author manuscript; available in PMC 2019 May 01.

Published in final edited form as:

J Leukoc Biol. 2018 May ; 103(5): 867–883. doi:10.1002/JLB.2A1017-407RR.

OXIDIZED LDL PHAGOCYTOSIS DURING FOAM CELL FORMATION IN ATHEROSCLEROTIC PLAQUES RELIES ON A PLD2-CD36 FUNCTIONAL INTERDEPENDENCE

Ramya Ganesan[1], **Karen M. Henkels**[1], **Lucile E. Wrenshall**[2], **Yasunori Kanaho**[3], **Gilbert Di Paolo**[4], **Michael A. Frohman**[5], and **Julian Gomez-Cambronero**[1,*]

[1]Department of Biochemistry and Molecular Biology, Wright State University, Dayton, OH

[2]Department of Neuroscience, Cell Biology/Physiology, Wright State University, Dayton, OH

[3]Department of Physiology, University of Tsukuba, Japan

[4]Department of Pathology and Cell Biology, Columbia University (Present address: Denali Therapeutics Inc., South San Francisco, CA)

[5]Department of Pharmacology, School of Medicine, Stony Brook University, NY

Abstract

The uptake of cholesterol carried by Low Density Lipoprotein (LDL) is tightly controlled in the body. Macrophages are not well suited to counteract the cellular consequences of excess cholesterol leading to their transformation into “foam cells”, an early step in vascular plaque formation. We have uncovered and characterized a novel mechanism involving phospholipase D (PLD) in foam cell formation. Utilizing bone marrow-derived macrophages from PLD genetically-deficient mice, we demonstrate that PLD2 (but not PLD1)-null macrophages cannot fully phagocytose aggregated oxidized LDL (Agg-Ox-LDL), which was phenocopied with with a PLD2-selective inhibitor. We also report a role for PLD2 in coupling Agg-oxLDL phagocytosis with WASP, Grb2 and Actin. Further, the clearance of LDL particles is mediated by both CD36 and PLD2, in a mutual dependence on each other. In the absence of PLD2, CD36 does not engage in Agg-ox-LDL removal and when CD36 is blocked, PLD2 cannot form protein-protein heterocomplexes with WASP or Actin. These result translated into humans using a GEO database of microarray expression data from atheroma plaques versus normal adjacent carotid tissue and observed higher values for NFkB, PLD2 (but not PLD1), WASP and Grb2 in the atheroma plaques. Human artherectomy specimens confirmed high presence of PLD2 (mRNA and protein) as well as phospho-WASP in diseased arteries. Thus, PLD2 interacts in macrophages with Actin, Grb2 and WASP during phagocytosis of Agg-ox-LDL in the presence of CD36 during their transformation into “foam cells”. This knowledge provides several new molecular targets to better understand the disease and counteract vascular plaque formation.

*Corresponding author: Julian Gomez-Cambronero, Ph.D., Department of Biochemistry and Molecular Biology, 3640 Colonel Glenn Highway, Wright State University School of Medicine, Dayton, Ohio 45435, Ph: 937-775-3601 | julian.cambronero@wright.edu, http://people.wright.edu/julian.cambronero.

The authors declare no conflicts of interest. All authors have made substantial contributions to the conception and design of the study, or acquisition of data, or analysis and interpretation of data; to the drafting the article or revising it critically for important intellectual content; and to the final approval of the version submitted.

Keywords

Leukocytes; Macrophages; Inflammation; Phospholipid; Phospholipase

INTRODUCTION

Atherosclerosis is an inflammatory disease of the vasculature that leads to the development of atheromatous plaques within vessel walls [1]. A key mechanism in plaque development involves migration and proliferation of vascular smooth muscle cells and macrophages. Phagocytosis, most commonly associated with cells of the innate immune system such as macrophages, is used to engulf and eliminate pathogens and damaged cells. Exaggerated macrophage phagocytosis of accumulating lipids in arterial walls leads to the formation and accumulation of foam cells. The phagocytosis proceeds through both receptor-dependent and - independent uptake of low density lipoprotein (LDL) [2]. LDL-laden foam cell formation of atheromatous plaques narrows arterial lumens, which can partially or completely restrict blood flow to the heart, brain (stroke) and limbs (peripheral arterial disease (PAD)). Ruptured plaques can also trigger strokes through the delivery of cellular-debris emboli to the brain.

Oxidatively-modified LDL (ox-LDL), consists of protein components that have been modified by aldehyde products that create net negative charges that render the ox-LDL very attractive to macrophages in terms of uptake (phagocytosis) specially when aggregated in large particles as Agg-Ox-LDL [3] and are prevalent in atheromatous plaques [4–7]. Monocytes differentiated into macrophages with M-CSF phagocytose aggregated, oxidized LDL (Agg-Ox-LDL) in large quantities [5–7]. This process is more prevalent in the arterial wall due to macrophage-secreted proteoglycan [8]. Macrophage foam cell formation requires Agg-Ox-LDL and neutralization of the CD36 receptor, in other words, is a process that involved CD36 receptor-mediated uptake of Ox-LDL [9]. The molecular and genetic mechanisms that govern macrophage phagocytosis of LDL and hasten inflammation are still unknown in terms of vascular biology. Until we understand these processes, therapeutic or surgical approaches used to disrupt/remove plaque will have suboptimal long-term outcomes, as the process of macrophage/foam cell formation will start again.

An underlying, chronic inflammation is responsible for the development and continued progression of atherosclerosis [10], which is a significant health problem and a major contributor to cardiovascular disease (CVD). Atherosclerosis accounts for one in three deaths in the U.S. [11], continues to rise globally [12–14], and is a major contributor to current healthcare costs [11]. Thus, it is very important to limit or terminate inflammation and start vascular healing early on. Plaque growth and swelling in a diseased artery involves migration of immune cells and the conversion of macrophages into foam cells [15]. Accumulation of ox-LDL in macrophage-derived foam cells directly affects foam cell migration and increases focal adhesion kinases (FAK), which drives foam cell accumulation in the arterial intima leading to atheromatous plaque formation [16].

FAK signaling pathways heavily implicated in inflammation, cell migratory processes, and macrophage podosome and phagocytic cup formation include Phospholipase D (PLD),

Wiskott-Aldrich Syndrome protein (WASP) and Actin polymerization [17–22]. PLD catalyzes the breakdown of the phospholipid phosphatidylcholine into phosphatidic acid (PA) and choline [23, 24]. PLD plays a key role in neutrophil and macrophage-initiated inflammation in many disease states, including chronic inflammation and cardiovascular disease, due to its involvement in signaling pathways promoting cell growth, proliferation and migration [25–27].

Studies using PLD knockout (KO) mice or chemical inhibitors have reported that suppressing PLD is “protective” during ischemic stroke [28], hypertension [29], thrombosis [30, 31] and myocardial infarction [32]. WASP has a poly-proline rich region, a polybasic region, and a GTPase Binding Domain and is a key regulator in the formation of phagocytic cups [33–39]. WASP binds to cofilin and the Arp2/3 complex through its C-terminal activity (Verprolin-Cofilin-Acidic, VCA) region to polymerize actin monomers (G-actin) into F-actin. Previously, our laboratory showed that the Phospholipase D2 isoform (PLD2) has a signaling role in WASP-mediated macrophage phagocytosis and phagocytic cup formation [40]. Defining a direct protein-protein interaction between PLD2-WASP in foam cells within the plaque is a novel approach that could potentially help to explain excessive phagocytosis of ox-LDL.

In this study, we used either macrophages differentiated from PLD knockout mice or the newest generation of PLD isoform-specific small molecule inhibitors [25, 28, 41] to inhibit macrophage foam cell phagocytosis. We report herein that macrophages phagocytose plaque cholesterol and undergo foam cell formation less efficiently in the absence of PLD2, suggesting a role for it *in vivo* in development of vascular inflammation and atheromatous plaques in the clinical setting.

METHODS

Materials

RAW264.7 mouse macrophages (cat. # TIB-71) and DMEM (cat. # 30-2002) were obtained from ATCC (Manassas, VA, USA). RPMI 1640 with L-glutamine and 25 mM HEPES (cat. # SH30255.01) and ECL reagent (cat. # RPN2106) were from GE Healthcare Life Sciences (Logan, UT, USA). Fetal bovine serum (heat inactivated) (cat. # 900-108) and Penicillin/Streptomycin (10,000 units penicillin/10,000 mg/ml streptomycin) (cat. # 400-109) were from Gemini Bio-Products (West Sacramento, CA, USA). Oxidized LDL (cat. # L34357) were from Life technologies (Carlsbad, CA) that was further oxidized with 20 μM copper. Sterile-filtered Histopaque 1077 (cat. # 10771), sterile-filtered Histopaque 1119 (cat. #11191) and Oil Red O stain (1-(2,5-dimethyl-4-(2,5-dimethylphenyl) phenyldiazenyl) azonapthalen-2-ol) (cat. # O0625) were from Sigma-Aldrich (St. Louis, MO, USA). 0.5 M EDTA, pH 8.0 (cat. # 15575-038) was from Life Technologies (Carlsbad, CA, USA). Recombinant mouse M-CSF (cat. # 315-02) was from PeproTech (Rocky Hill, NK, USA). CD36 blocking antibody (cat. # ab23680) was obtained from Abcam (Cambridge, MA). Mouse isotope control antibody (cat. # 553476) was obtained from BD Biosciences (San Diego, CA).

Animals

Bone marrow-derived macrophages (BMDMs) were obtained from male or female wild-type (Charles River Laboratories, Charleston, SC, USA). PLD1$^{-/-}$ were generated at Dr. Yasunori Kanaho's laboratory, University of Tsukuba, Tennodai, Japan [42]. These PLD1-KO c57BL/6 mice had initially PLD2 in ES with exons 13 removed [42]. PLD2$^{-/-}$ were generated at Dr. Gilbert Di Paolo's laboratory, Columbia University [43]. These PLD2-KO c57BL/6 mice had initially PLD2 in ES with exons 13–15 removed [43]. Wild type mice were also in the C57Bl/6 background at 6–8 wks of age (weighing 20–25 g) comparable to the KOs. The mice were provided a temperature- and light-controlled environment with unrestricted access to food (laboratory standard rodent diet 5001 (Laboratory Diet, St. Louis, MO, USA)) and water. The mice had veterinary care, were checked ever day, and experiments were performed in accordance with the Wright State University (WSU) Institutional Animal Care and Use Committee (IACUC) guidelines. Experiments for this manuscript have also followed the National Institutes of Health guide for the care and use of Laboratory animals (NIH Publications No. 8023, revised 1978).

Isolation of bone marrow-derived macrophages (BMDM)

Bone marrow from WT, PLD1$^{-/-}$ and PLD2$^{-/-}$ euthanized mice was extracted from femurs and tibias according to [44]. The bones were washed once in 70% ethanol and then twice in 1× PBS. The epiphyses (ends of the femur and tibia) were cut carefully with a new, single-edge razor, and then, using a 12 cc syringe and 25 G × 5/8 in. needle, RPMI media with 10% FBS and 2mM EDTA was used to flush out the bone marrow cells, which were passed through a 100 mm cell strainer placed on top of a 50 ml conical tube. This step was repeated from the other end of the bone to obtain the maximum number of cells possible. The bones were then cut into pieces, placed on top of the cell strainer, and crushed with the back of the syringe to recover any remaining cells. The cells were then sedimented at 1400 rpm for 7 min at 4 °C, resuspended in 1× PBS, and counted. Cells were allowed to settle in the centrifuge tube and then the supernatant media carefully aspirated. The cells were resuspended in 20 ml of 0.2% NaCl to lyse red blood cells and incubated for 20 seconds. 20 ml of 1.6% NaCl was then added and the cells sedimented at 1400 rpm for 7 min at 4°C. The pellet was resuspended in 1ml RPMI media with 10% FBS and 2mM EDTA, centrifuged at 1400 rpm for 7 min at 4 °C, and resuspended in 1 ml of RPMI media with 10% FBS and 100 ng/ml M-CSF.

Differentiation of bone marrow cells into BMDM

Bone marrow cells were plated at a density of 2.0–2.5 × 10^7 cells/plate in 100 mm tissue culture-grade plates. Media was changed on Day 3 and again on Day 6 with RPMI-1640, 10% FBS, Pen-Strep, and 100 ng/ml M-CSF. On Day 7, the BMDM were washed twice with PBS and harvested by incubation in 10 ml PBS containing 10 mM EDTA, followed by vigorous pipetting using complete RPMI media with 100 ng/ml M-CSF. The BMDM were sedimented at 250×g for 5 min and counted using a hemocytometer.

Preparation of aggregated, oxidized LDL particles (Agg-Ox-LDL)

Extensively oxidized LDL can interact with phagocytic cells [45, 46] leading to delivery of LDL to macrophages by phagocytosis and subsequent formation of foam cells [47]. LDL aggregation and fusion are important early steps in atherogenesis [48]. As LDL oxidation increases aggregation [49–51], we used 20 μM copper-highly oxidized LDL (cat. # L34357) from Life technologies (Carlsbad, CA) at an initial concentration of 1 mg/ml. Extent of aggregation was monitored by absorbance (turbidity) at 680 nm before each experiment. However, physical properties of Agg-oxLDL were measured initially for each batch in a NanoSight NS300 with a 405 nm laser instrument (Malvern Instruments, United Kingdom). A typical measurement indicated that the mean size of the particles was 138 +/− 6.0 nm and 90% of the particles had sizes of 212 nm +/− 1.2 or below. Since size of single-molecule, non-oxidized LDL is only ~20 nm, we call our preparations for the experiments “aggregated, oxidized LDL” (Agg-Ox-LDL).

Phagocytosis of Agg-Ox-LDL by macrophage foam cells

BMDM from c57BL/6 mice or were differentiated into macrophages by continuous culture with 100 ng/ml M-CSF [52]. RAW264.7 macrophages were incubated as we have described in [25–27]. Cells were plated in a 12-well plate at a density of 2.5×10^5 cells/well and allowed to grow overnight in a humidified 37 °C incubator. Agg-Ox-LDL were added to the wells (0, 50 or 100 μg/ml) for 24h or 48h after which the media was aspirated and the cells washed in 1× PBS. Foam cells were fixed in 4% paraformaldehyde, washed with 1× PBS, and then incubated twice with 1 ml of 100% propylene glycol for 5 min each time. The supernatants were aspirated and the cells stained with 1 ml of 65 °C Oil Red O for 1 h. The stain was aspirated and the cells washed with 85% propylene glycol for 3 min followed by 2× in distilled water. The cells were counter-stained using hematoxylin for 2 min and washed 7× with water. After air drying, photomicroscopic imaging was conducted using an EVOS microscope (40× magnification). Oil Red O-stained foam cells were quantified in terms of fold-difference compared to control samples [4, 7]. Foam cell formation was measured using Image J. The bright-field images were opened and scale was set to 200 μm. The images were then set to grayscale using RGB stack, with threshold set to half the maximum threshold. The images were then analyzed by clicking measure to obtain the intensity of oil red staining [53].

Phagocytosis of Zymosan

Macrophage phagocytosis was performed as per prior studies [40, 54]. Briefly, phagocytosis was measured using phRhodo Red zymosan (Life Technologies, Carlsbad, CA, USA). The particles were resuspended in live cell imaging solution (Invitrogen, Carlsbad, CA, USA) to a final concentration of 50×10^6 particles/ml and sonicated and added to 1×10^5 macrophages in the ratio of 1:50 (cells:particles) in 24-well tissue-culture treated plates. The 24-well plates containing the cells and zymosan were incubated at 37 °C for 2 hr. phRhodo Red zymosan particles ingested by macrophages were measured using a Gen 5.0 plate reader at 560/585 (excitation/emission) nm.

Immunofluorescence microscopy of phagocytosis key proteins

Macrophage foam cells were incubated with Agg-Ox-LDL in a time-course experiment to measure phagocytic cup formation, similar to [40]. Samples were fixed, permeabilized, blocked and then incubated with fluorescent antibodies specific to WASP, Grb2 and PLD2 using AlexaFluor350-, FITC- or TRITC-labeling of two out of the three total proteins at any one time, allowing us to visualize fluorescent Agg-Ox-LDL and two target proteins [40, 55]. Photomicrographs at 100× magnification were rendered using a Nikon Eclipse 50i inverted fluorescence microscope, Infinity2 Lumenera digital camera and Infinity Analyze software (v. 6.2). The immunofluorescence co-localization of protein pairs was quantified using ImageJ software with ~2–4 cells per field; 6 fields; n=3 independent experiments, by determining the Pearson's coefficient [56, 57], which was then plotted as % of co-localization (yellow=TRITC-PLD2 and FITC-Grb2; or TRITC-PLD2 and FITC-Actin; or TRITC-PLD2 and FITC-WASP).

Human artery specimens

Our IRB protocol number is SC 5561 (Wright State University School of Medicine, Dayton, Ohio). Small sections of normal human artery and popliteal vein controls, and also diseased popliteal artery and plaque from ileofemoral endarterectomy were obtained from deceased donor organs. Consent for research with the obtained tissue was by next of kin. Tissues were obtained and either flash-frozen or stored in formalin. The formalin fixed-tissue samples were used for sectioning for Immunofluorescent staining or tissue histology H&E staining (AML Laboratory Inc., FL). The flash-frozen sections were further processed with lysis buffer containing collagenase and phosphatase inhibitors by homogenization and ultrasonication for western blot analysis after SDS-PAGE or gene expression analysis (qRT-PCR).

Gene expression measurement

Relative mRNA gene expression levels were measured by Quantitative Real time PCR (qRT-PCR). Total RNA was isolated from cells with the RNeasy minikit. RNA concentrations were quantified using the NanoDrop ND-1000 UV/Vis spectrophotometer and samples were normalized to 2 μg RNA. Reverse transcription was performed with 2 μg RNA, 210 ng random hexamers, 500 μM dNTPs, 84 units RNaseOUT, and 210 units of SuperscriptII reverse transcriptase and incubated at 42 °C for 55 minutes. Q-PCR reactions were run with 100 ng total input RNA, 1 μl (which contained 250 nM of the probe and 900 nM of the primers) of either FAM-labeled PLD1 (Hs00160118_m1 Cat#: 4331182) or FAM-labeled PLD2 (Hs01093219_m1 Cat#: 4351372) gene expression assay multiplexed with the FAM-labeled housekeeping genes Actin (Hs01060665_g1 Cat#: 4331182), GAPDH (Hs02758991_g1 Cat#: 4331182), and TATA-Binding protein (TBP) (Hs00427621_m1 Cat#: 4331182). qRT-PCR conditions for the Stratagene Mx3000P were: 95 °C for 3 min and then 40 cycles of the next 3 steps: 30 s 95 °C, 1 min 60 °C, and then 1 min 72 °C. The "cycle threshold" Ct values were arbitrarily chosen from the linear part of the PCR amplification curve where an increase in fluorescence can be detected >10 S.E.M. above the background signal. ΔCt was calculated as: ΔCt = Avg. PLD Ct − Avg. Housekeeping Ct; and gene fold expression, as $2^{-(\Delta\Delta Ct)} = 2^{-(\text{experimental Condition } \Delta Ct - \text{Control } \Delta Ct)}$. We

calculated the Ct ratios of experimental condition/housekeeping gene: TATA Binding Protein (TBP).

Computational transcriptomic analysis

For the data presented in Figure 1, we used gene expression data from the human carotid artery atheroma study included in the NCBI Gene Expression Omnibus (GEO) microarray dataset [58]. We chose this study as it included carotid artery atheromatous plaque samples from hypertensive human patients compared to control companion healthy artery tissue. We used data from a single study to assure that it was generated using similar methodologies. The study we chose had 34 pairs of normal, adjacent carotid tissue and atheroma plaque. Per Ayari *et al.*, gene expression values were scaled logarithmically [58]. All of the data from the genes of interest were downloaded to MS Excel spreadsheets from GEO during July 2016. Genes were defined as being over- or underexpressed when the fold-change in the atheroma plaque group was significantly different compared to the adjacent normal carotid tissue ($p<0.05$). Results were analyzed using GraphPad Prism 6.0 (GraphPad Software, San Diego, CA, USA). Unpaired t-tests were used to compare gene expression data.

PLD inhibitors

The PLD inhibitors VU0155069 (selective for PLD1), that has an IC_{50} of 9 nM [59], VU0364739 (also called NFOT; selective for PLD2) that has an IC_{50} of 10 nM [59], and FIPI (a dual PLD1/2 inhibitor) [60] that has an IC_{50} of 10 nM for PLD1 and 8 nM for PLD2 [59], were added to the cell cultures at 700 nM for 30 mins prior to initiating experiments. We studied the effect of PLD inhibitors on foam cell formation after 24 h by Oil-red O staining.

SDS-PAGE and Western blot analyses

To confirm the presence of the proteins of interest in the human artery samples, we performed SDS-PAGE and western blot analyses specific for these proteins, as well as for actin as a protein loading control. Approximately 150 μg of protein lysate was loaded per lane. For western-blot analyses, rabbit anti-PLD1 (F-12) IgG (Santa Cruz Biotechnology, Santa Cruz, CA, USA) (cat. # sc-28314), rabbit anti-PLD2 (N-term) IgG (Abgent, San Diego, CA, USA) (cat. # AP14669a), rabbit anti-WASP IgG (D9C8) (Cell Signaling Technology, Danvers, MA, USA) (cat. # 4271), rabbit anti-phospho-WASP (phospho Y290) (Abcam, Cambridge, MA, USA) (cat. # ab59278), mouse anti-Grb2 IgG (3F2) (EMD Millipore, Billerica, MA, USA) (cat. # 05-372) and rabbit anti-Actin (13E5) IgG (Cell Signaling Technology) (cat. # 4970) were utilized as primary antibodies according to the manufacturers' recommendations. Anti-rabbit IgG HRP antibodies were from Cell Signaling Technology (cat. # 7076). Immunoreactivities were detected using enhanced chemiluminescence (ECL) reagents from GE Healthcare (Pittsburgh, PA, USA) (cat. # RPN2106) and autoradiograph film.

Co-immunoprecipitation

RAW264.7 cells were cultured in reduced bicarbonate DMEM plus 10% fetal bovine serum. The plasmids used for transfections were pcDNA3.1-mycPLD2-WT, pcDNA3.1-XGrb2 and

pEGFP-C1-WASp. When cultured cells reached a confluence of 60%, they were transfected with the plasmid of interest. Transfections were performed using 5 μl Superfect (Qiagen, Valencia, CA, USA) in Opti-MEM media previously mixed in sterile glass test tubes. The DNA and Superfect were mixed in post-transfection media (without antibiotics), applied to cells, and then transfected for 36 h. After transfection, the cells were harvested and lysed with Special lysis buffer (5 mM HEPES, pH 7.8, 100 μM sodium orthovanadate, and 0.1% Triton X-100 and protease inhibitors (aprotinin 2 μg/ml and leupeptin 5 μg/ml). The lysates were sonicated and treated with 1 μl monoclonal antibody for the respective protein and 10 μl agarose beads (Millipore, Billerica, MA) and incubated at 4 °C overnight. After incubation, the immunoprecipitates were washed with LiCl wash buffer (2.1% LiCl, 1.6% Tris-HCl, pH 7.4) and NaCl wash buffer (0.6% NaCl, 0.16% Tris-HCl, 0.03% EDTA, pH 7.4), respectively, and sedimented at 12,000 × g for 1 min. The resulting pellets were then analyzed using SDS-PAGE and Western blotting (WB).

Statistical Analysis

Data presented in the Figures as bars are means + Standard Error of the Mean (SEM) (standard deviation/n1/2, were n is the sample size). Experiments were performed in technical triplicates (for qPCR assays) or technical duplicates (for PLD activity assays) for n=5 independent experiments. The difference between means was assessed by the Single Factor Analysis of Variance (ANOVA) test or paired t-test, calculated using Prism 7 (Graphpad software Inc., La Jolla, CA). Probability of $p<0.05$ indicates a significant difference. In the figures, the (*) symbols above bars denote statistically significant ($P<0.05$) ANOVA or t-test increase or decrease between samples and controls.

RESULTS

Macrophage phagocytosis of Agg-Ox-LDL is reduced in the absence of PLD2 activity

Based on earlier work from our laboratory that outlined the importance of PLD in macrophage phagocytosis and phagocytic cup formation [40, 61, 62], we examined the potential requirement of PLD for the ability of macrophages to differentiate into Agg-Ox-LDL-laden foam cells. Cholesterol can be taken up by macrophages by receptor-mediated processes (chiefly CD36 scavenger receptor), pinocytosis or phagocytosis. To ensure that we studied here phagocytosis, we prepared aggregated, oxidized LDL particles (Agg-Ox-LDL) of ~140 nm Mean size as detailed in Methods and shown in Figure 1A, whose large size is optimized for phagocytosis. At least 90% of the ox-LDL particles are between 50–250 nm in diameter. Considering that one LDL particle is around 20 nm, our preparations were aggregates. In fact, PLD2 is weakly activated with non-aggregated particles (data not shown).

Bone marrow-derived monocytes from wild-type (WT) and PLD1- and PLD2-deficient mice were differentiated into macrophages [52] and then stimulated to undergo foam cell formation by incubation with 50 μg/ml aggregated, oxidized LDL (Agg-Ox-LDL) cholesterol [50, 63]. We used BMDMs because they are uniformly quiescent until stimulated, whereas intraperitoneal macrophages are activated to varying levels. Foam cell

formation was monitored by staining for macrophage internalization of Agg-Ox-LDL using Oil Red O, a fat-soluble dye that binds to neutral triglycerides and lipids [64, 65].

Foam cells have an enlarged, red appearance in comparison to the relatively smaller, pale-colored macrophages (Fig. 1B). WT and PLD1$^{-/-}$ macrophages both readily took up Agg-Ox-LDL and formed foam cells to similar extents as determined by visual inspection (Fig. 1C) and were not significantly different in uptake based on quantitation (Fig. 1D). In contrast, PLD2$^{-/-}$ macrophages phagocytosed significantly less Agg-Ox-LDL compared to WT mice and formed foam cells at a reduced frequency over the time-course of the assay (Fig. 1C,D). Data in Fig. 1D indicates that the absence of PLD1 provokes a reduction of ~27% in phagocytosis (compared with WT), whereas the absence of PLD2 provokes a reduction of >60%. Since the reduction in the first case was small and within the margin of SEM of WT, we considered the involvement of PLD2 as more robust. Further, we believe that the physiological reason for a larger participation of PLD2 is because this isoform has been found in the plasma membrane [66] and cytosol, while PLD1 is localized in the ER and Golgi membranes [67]. Thus, PLD2 would appear to be more important for cytoskeletal rearrangements during active phagocytosis of ox-LDL as it is localized at the plasma membrane.

For controls of macrophage phagocytosis, we performed experiments where bone marrow derived macrophages (BMDM) from WT, PLD1-KO or PLD2-KO were presented with phRhodo Zymosan for phagocytosis. Figure 1E indicates a reduced rate of phagocytosis when PLD2 isoform is knocked out. This is in line with well-known results of regulates macrophage phagocytosis. Thus, whereas BMDM needed both PLD1 and PLD2 for general phagocytosis, those cells relied heavily on PLD2 to mediate phagocytosis of Agg-Ox-LDL for formation of foam cells, which is a novel result presented herein.

PLD inhibitors reduce Agg-Ox-LDL phagocytosis

PLD2 interacts with many different proteins and has been proposed in some contexts to have non-catalytic roles [68]. To address whether PLD activity is key for Agg-ox-LDL phagocytosis, we investigated the ability of small molecule PLD inhibitors to reduce Agg-Ox-LDL uptake from macrophages. WT macrophages were cultured in media containing inhibitors that block activity of both PLD1 and PLD2 (FIPI) [60], and relatively selective for PLD1 NBOD (VU0155069) [26, 69], or selective for PLD2 NFOT (VU0364739). Agg-Ox-LDL uptake by macrophages was significantly inhibited by all three inhibitors, with the PLD2-selective inhibitor (VU0364739) being the most potent and the PLD1-selective inhibitor (VU0155069) being the least potent (Fig 2A). At 700nM VU0155069, the highest concentration that significantly inhibited uptake, PLD2 is also partially inhibited [69], suggesting that PLD1 may have a weak if any role in the phagocytosis observed.

To test if Agg-Ox-LDL phagocytosis had any component mediated by scavenger receptor CD36 [70–72], which signals through Src and Jnk2 [73–75], we generated BMDM from WT, PLD1 and PLD2 mice and blocked CD36 using a monoclonal antibody during culture of the cells with Agg-Ox-LDL. The CD36 antibody was effective in reducing Agg-Ox-LDL uptake for WT and PLD1$^{-/-}$ BMDMs. Blocking CD36 in WT and PLD1-KO (in both cases PLD2 is still present), ingestion of ox-LDL was reduced to levels equivalent to PLD2-KO,

indicating that CD36 is needed for the clearance of thee particles. However, CD36 antibodies did not reduce uptake by PLD2$^{-/-}$ BMDMs beyond the suppression already created by the absence of PLD2 (Fig. 2B). Thus, in the absence of PLD2, CD36 does not seem to engage in ox-PLD removal. Additionally, whatever low level of uptake was observed in PLD2-KO cells (putatively due to PLD1 or other pathways) was found further reduced when the cells were incubated with cytochalasin D (Fig. 2B), a well-known cytoskeleton disruptor and phagocytosis inhibitor. Both these results (anti-CD36 antibody and cytochalasin D), along with the fact that we used in the experiments Agg-Ox-LDL (particles ~10× larger in diameter than individual LDL molecules) indicate that the uptake occurred through phagocytosis mediated by both CD36 and PLD2. Further experiments described below confirmed the new PLD2-regulated pathway.

The heterotrimeric protein complex of PLD2-Grb2-WASP

PLD2, through its product phosphatidic acid (PA), which mediates cell migration of macrophages and neutrophils [76, 77]. This signaling pathway is also dependent on Wiskott-Aldrich syndrome protein (WASP) (a crucial protein needed for actin polymerization and, as such for phagocytosis) and on Growth factor receptor-bound protein 2 (Grb2), with Grb2 functioning as the docking protein that mediates the physical interaction between PLD2 and WASP (Fig. 3A). The SH2 domain of Grb2 interacts with the Y169 and Y179 residues of PLD2, while the two SH3 domains of Grb2 interact with the polyproline region of WASP. This heterotrimeric protein binding interaction is dependent on phosphatidic acid (dioleoyl-PA), as macrophages incubated in the presence of 300 nM dioleoyl-PA exhibited increased interaction of PLD2-Grb2-WASP as a function of time, as shown using co-immunoprecipitation (Fig. 3B). A recent study has shown that exogenously-supplied PA can be detected by a PA sensor inside cells during phagocytosis [78]. Moreover, from previous studies in our laboratory, we know that exogenously-supplied PA activates PLD (to mimic activated PLD), resulting in increased activity and downstream cellular signaling cascades [79, 80].

To investigate whether the same proteins are involved in Agg-Ox-LDL phagocytosis by macrophages, we used 50 μg/ml Agg-Ox-LDL to induce BMDM cells to form foam cells and performed immunofluorescent immunostaining to visualize PLD2, Grb2, WASP and Actin localization. The results are broken in the study of interactions of two proteins at the time. We first asked if a Grb2-PLD2 interaction could be detected in IF as it was in IP/WB (Fig. 3B). As presented in Figure 3C,D, in the absence of Agg-Ox-LDL in the cell cultures, Grb2 and PLD2 did not visually co-localize. In Fig. 3C, the red (PLD2-TRITC) and green (Grb2-FITC) signals are distinct, as pointed by arrowheads. In contrast, with Agg-Ox-LDL treatment, PLD2 broadly co-localized with Grb2 in WT and PLD1-KO BMDMs. This was evidenced by the yellow fluorescence as indicated by the arrows and it was properly quantified as indicated in Methods and data presented in Figure 3D.

A putative PLD2 interaction with Actin was next studied. Co-localization of these two proteins increased substantially with Agg-Ox-LDL treatment (Fig 4A, first row and quantification, Fig. 4B, first two bars on the left). In order to further study a possible role of CD36 in this protein-protein (PLD2-Actin) interaction during foam cell formation, we

incubated cells with monoclonal anti-CD36 antibodies to block the CD36 receptor action, and then subjected the cells to Agg-Ox-LDL treatment. The results (Fig 4A, quantification Fig. 4B, third bar on the left) showed that the PLD2-Actin co-localization was negated by the CD36 antibody, indicating the importance of CD36 in the formation of the PLD2-Actin interaction for ox-LDL phagocytosis. That the presence of PLD2 is crucial is shown in Fig. 4A, second row (and quantification, Fig. 4B, last three bars) in PLD2-KO BMDMs, that yielded no change in the localization pattern for PLD2 and Actin in the presence or absence of Agg-Ox-LDL, albeit the cells were consistently smaller than WT controls.

A PLD2 interaction with WASP by immunofluorescence (already detected in IP/WB, Figure 3B) was next studied. Co-localization of these two proteins increased moderately with Agg-Ox-LDL treatment and this was negated with anti-CD36 antibodies (Fig. 4C, quantification Fig. 4D). As in the PLD2-Actin experiments, the presence of PLD2 is crucial as no localization is seen in PLD2-KO BMDM (Fig 4A–D). Taken the findings in Figures 3 and 4 together, it can be concluded that mediation of a phospholipase identified as a molecular mechanism by which macrophages become foam cells *in vivo* in atherosclerotic plaques where in PLD2 complexes with Actin, Grb2 and WASP during phagocytosis of ox-LDL and that the presence of CD36 is important for the formation of the protein complexes.

Arterial gene expression during atherosclerosis

To pursue clinical correlates, we mined gene expression profiles of PLD and some of its key signaling protein partners in a human disease that relies heavily on macrophage function and signaling. Through comparing relative mRNA expression levels in human atheroma plaque tissue and adjacent, non-diseased carotid artery samples, using the Carotid Artery Atheroma Dataset at the Gene Expression Omnibus (GEO) microarray (accession number GDS5083) [58], we determined that that NFκB1 (used here as a general marker of inflammation), PLD2, WASP and Grb2 ($p=0.0016$, $p=0.005$ and $p<0.0001$, respectively) undergo upregulation in diseased vascular tissue (Fig. 5A–D). NFkb1 represented a positive control, as it is a well-known marker of inflammation. In contrast, there was no change in expression of PLD1 (Fig. 5E, $p=0.24$), further supporting its lack of relevance in this disease context.

PLD2 but not PLD1 is upregulated in diseased artery tissues –A translational study

To confirm that hypoxic conditions actually do trigger PLD expression in diseased human artery and atheromatous plaques, we used human undamaged control and diseased atherosclerotic artery specimens to assess both relative mRNA and protein expression levels. We performed quantitative RT-PCR and/or SDS-PAGE/western blot analyses on human patient samples and measured the expression levels of PLD, Grb2 and WASP. We analyzed samples for both PLD isoforms and found that while PLD2 mRNA was significantly upregulated in the diseased artery and plaque samples (Fig. 6A), PLD1 mRNA was virtually undetectable (Fig. 6B). Similar findings were observed for PLD2 and PLD1 protein expression levels by western blot (Fig. 6C); PLD2 was upregulated in the diseased artery samples that contained atherosclerotic plaque (both from diseased femoral artery and ileofemoral endarterectomy), while PLD1 was downregulated.

Upregulation of Wiskott-Aldrich Syndrome protein (WASP) and Grb2 in diseased artery tissues

We similarly investigated the expression of WASP and Grb2 in human undamaged control and diseased atherosclerotic artery specimens. WASP and Grb2 protein expression levels were increased in the diseased artery samples compared to the non-diseased companion tissues (Fig. 6C–D). Furthermore, WASP activation was increased, as assessed by detecting phosphorylation at the WASP tyrosine residue 290, using a phosphotyrosine-specific antibody (Fig. 6C–D). These data suggest a role for activation of WASP protein in the diseased artery and plaque samples, which could play a role in membrane-associated actin polymerization at the leading edge of phagocytic arms involved in phagocytosis of Agg-Ox-LDL and foam cell formation.

Validation of PLD2, WASP and Grb2 in diseased human artery samples

Formalin-fixed companion samples to those diseased tissues shown in the Fig. 6 mRNA and protein expression assays were used for H&E staining and immunofluorescence microscopy (IF). As shown in Fig. 7A, H&E staining revealed positive staining in the diseased artery towards the lumen, adjacent to but not in the acellular area. The positive staining in the plaque, which is from the same vessel, looks contiguous with the staining in the diseased artery, and that area is not highly cellular (based on DAPI). PLD1 IF staining of tissues with rabbit α-PLD1-FITC-conjugated IgG antibodies showed little-to-no PLD1 expression in the plaque and endarterectomy arteries, similar to the diseased artery alone (Fig. 7B).

In contrast, immunofluorescence staining of these tissues using rabbit α-PLD2-FITC-conjugated IgG antibodies indicated that PLD2 expression is concentrated in the plaque in diseased arteries (Fig. 7C) and in the plaque that was removed during endarterectomy when compared to the diseased artery alone. The positive PLD2 staining in the diseased artery (Fig. 7C, left panel) appears to be towards the lumen. The positive staining in the plaque (Fig. 7C, middle panel), appears to be adjacent to the staining in the diseased artery. Thus, PLD2 appears in the area of the plaque underneath the fibrous cap.

DISCUSSION

Phospholipase D and its catalytic product PA have been linked to cell signaling, cell proliferation, inflammation and cancer. Phospholipase D (PLD) is a major signaling component in myeloid leukocytes cells where it plays a key role in cytoskeletal actin polymerization and phagocytosis where both isoforms, PLD1 and PLD2 coordinately regulate macrophage phagocytosis [40, 81]. The findings reported in this study center on macrophage phagocytosis of aggregated, oxidized-LDL and their conversion into foam cells. The data suggest PLD2-specific mechanism in foam cell formation, which is a key step in the progression of atherosclerosis.

Chronic inflammation is responsible for the development and continued progression of atherosclerosis [10], which encompasses a great portion of current healthcare costs [11]. Thus, it is very important to limit or terminate inflammation and start vascular healing. Plaque growth and swelling in a diseased artery involves migration of immune cells and the

conversion of macrophages into foam cells [15]. In atheroma formation, cholesterol in the form of LDL accumulates in the intima layer of arteries. The plaque is a complex mixture of cholesterol crystals, extracellular matrix, smooth muscle cells, endothelial cells, monocytes, macrophages and foam cells [82, 83]. Macrophages are recruited to the LDL accumulation and attempt to clear it. Foam cell formation occurs as a result of phagocytosis or uptake of Agg-Ox-LDL, causing cholesteryl ester accumulation in these cells [84–86]. Although much is known about cholesterol uptake by macrophages, what role PLD might have in phagocytosis of Agg-Ox-LDL is less clear.

The findings reported here are a substantial departure from the status quo of eliminating the plaque in atheroma and instead defines an entirely new angle of approaching the problem, which is to avoid formation of functional foam cells. The proposed research strategy shifts existing paradigms by characterizing a heretofore-unsuspected link between PLD2 and the progression of inflammation in atherosclerosis. We identified that PLD2 makes macrophage phagocytose Agg-Ox-LDL to form foam cells more efficiently in a process that is dependent on mechanism that PLD-Grb2-WASP. Other studies have shown that PLD2 regulates RGS2 expression in foam cell formation [87], but a direct role of PLD in foam cell formation has not been shown to date. We also know from previous studies that PLD2 plays an important role in receptor endocytosis [88]. Our study reveals that PLD2 not only regulates macrophage phagocytosis by phagocytic cup formation, but also promotes phagocytosis of Agg-Ox-LDL via CD36 (a Class B scavenger receptor). In line with previous studies emphasizing the role of PLD2 in receptor endocytosis, we found that absence of PLD2 CD36 mediated Agg-Ox-LDL uptake by macrophages during foam cell formation.

The data presented in this study support a key role for PLD2, as $PLD2^{-/-}$ macrophages phagocytose aggregated Ox-LDL (Fig. 1C–D) less efficiently than $PLD1^{-/-}$ macrophages and PLD2-specific inhibitors diminish phagocytosis (Fig. 2A). Gene and protein expression from diseased human artery and plaque samples indicate PLD2 but not PLD1 correlates with diseased vessels (Fig. 6). Thus, we have demonstrated that PLD2 plays a role in macrophage during foam cell formation whereas PLD1 does only marginally.

WASP is linked with actin polymerization, and we show that phospho-WASP is present in the atheromatous plaque removed during ileofemoral endarterectomy from diseased arterial samples (Fig. 6). Likewise, we also observed that PLD2 and Grb2 were upregulated in the diseased artery/plaque samples with very low basal expression in non-diseases artery (Fig. 6). We also know from other studies in the lab that hypoxia promotes macrophage PLD activity (data not shown). Based on this, we propose that once activated by hypoxia, PLD hastens the phagocytic capability of foam cells through a mechanism that involves PLD-Grb2-WASp interaction and subsequent actin remodeling to form phagocytic cups for Ox-LDL uptake by macrophages and consequently foam cell formation (Fig. 8).

Overall, we present a new paradigm: that CD36-PLD-Grb2-WASP heterotrimeric signaling axis in macrophages is a key mediator of macrophage phagocytosis of Agg-Ox-LDL and subsequent foam cell formation, as indicated in the Model presented in Fig. 8. We hypothesize that a mechanism for specific coupling between Agg-oxLDL and PLD2 could involve the negative curvature of PA in phagocytic arms or extensions of the phagocytic cup,

accounts for enhanced PLD activity and thus its role in CD36 uptake of Agg-Ox-LDL via receptor endocytosis. PLD is known for its role in inducing membrane curvature during leukocyte migration and phagocytosis [40, 89] as well as receptor endocytosis [66, 88].

This knowledge of a CD36-PLD-Grb2-WASP heterotrimeric signaling axis provides specific new protein targets in vascular biology that have potential implications for improving human health. The proposal that elevated PLD2, Grb2 and WASP expression/activation may support progression of the atherosclerosis is significant, as potent, new small-molecule inhibitors are currently available that could be used to pharmacologically inhibit foam cell formation.

According to the present study, using the PLD1-KO and PLD2-KO mice from references [42] and [43], respectively, the $PLD2^{-/-}$ macrophages do not take up Agg-Ox-LDL as well as WT macrophages do. However, it is entirely possible that they would eventually (meaning days or weeks, as atherosclerosis progresses slowly) take Agg-Ox-LDL up, permitting the formation of foam cells. Such delay in clearing would raise the local concentration of Agg-Ox-LDL in the extracellular space under the endothelial cells, which could help activate them to create a pro-inflammatory environment. There is always the intriguing possibility that time progression could cause a switch of the role of PLD from harmful to protective (or vice versa). In a related model of ischemia reperfusion indicate PLD1 found to be protective –when experiments are done after 28 days after initial reperfusion (chronic phase of reperfusion) [90]. It will be interesting to see what role PLD's isoforms would play in long-term studies by using ApoE/PLD double KOs.

Acknowledgments

The following grants to Dr. Cambronero (J.G-C.) have supported this work: HL056653-14 from the National Institutes of Health (NIH) and 13GRNT17230097 from the American Heart Association.

LIST OF ABBREVIATIONS

Ab	Antibody
Agg-oxLDL	Aggregated oxidized Low Density Lipoprotein
ANOVA	Analysis of the Variance
BMDM	Bone marrow-derived macrophages
CD36	Cluster of differentiation CD36 (scavenger receptor)
Ct	Cycle threshold
F-actin	filamentous actin
FITC	Fluorescein isothiocyanate
G-actin	monomeric actin
GEO	Gene Expression Omnibus microarray dataset
GFP	green fluorescent protein

Grb2	Growth factor receptor-bound protein 2
H&E staining	Hematoxylin Eosin staining
IF microscopy	Immunofluorescence microscopy
LDL	Low density lipoprotein
M-CSF	Macrophage colony stimulating factor
mRNA	Messenger RNA
PA	Phosphatidic acid
PLD	Phospholipase D
PLD1-KO	Phospholipase D1 Knockout
PLD2-KO	Phospholipase D2 Knockout
q-RT-PCR	Quantitative, real time, polymerase chain reaction
TRITC	Tetramethylrhodamine
WASP	Wiskott-Aldrich Syndrome protein
WT	Wild type

References

1. Paquissi FC. The role of inflammation in cardiovascular diseases: the predictive value of neutrophil-lymphocyte ratio as a marker in peripheral arterial disease. Ther Clin Risk Manag. 2016; 12:851–60. [PubMed: 27313459]
2. Johnson JL, Newby AC. Macrophage heterogeneity in atherosclerotic plaques. Current opinion in lipidology. 2009; 20:370–8. [PubMed: 19741337]
3. Parthasarathy S, Raghavamenon A, Garelnabi MO, Santanam N. Oxidized low-density lipoprotein. Methods in molecular biology. 2010; 610:403–17. [PubMed: 20013192]
4. Waldo SW, Li Y, Buono C, Zhao B, Billings EM, Chang J, Kruth HS. Heterogeneity of human macrophages in culture and in atherosclerotic plaques. The American journal of pathology. 2008; 172:1112–26. [PubMed: 18321997]
5. Aviram M, Maor I, Keidar S, Hayek T, Oiknine J, Bar-El Y, Adler Z, Kertzman V, Milo S. Lesioned low density lipoprotein in atherosclerotic apolipoprotein E-deficient transgenic mice and in humans is oxidized and aggregated. Biochemical and biophysical research communications. 1995; 216:501–13. [PubMed: 7488140]
6. Maor I, Hayek T, Hirsh M, Iancu TC, Aviram M. Macrophage-released proteoglycans enhance LDL aggregation: studies in aorta from apolipoprotein E-deficient mice. Atherosclerosis. 2000; 150:91–101. [PubMed: 10781639]
7. Zhao B, Li Y, Buono C, Waldo SW, Jones NL, Mori M, Kruth HS. Constitutive receptor-independent low density lipoprotein uptake and cholesterol accumulation by macrophages differentiated from human monocytes with macrophage-colony-stimulating factor (M-CSF). The Journal of biological chemistry. 2006; 281:15757–62. [PubMed: 16606620]
8. Schrijvers DM, De Meyer GR, Herman AG, Martinet W. Phagocytosis in atherosclerosis: Molecular mechanisms and implications for plaque progression and stability. Cardiovascular research. 2007; 73:470–80. [PubMed: 17084825]

9. Podrez EA, Febbraio M, Sheibani N, Schmitt D, Silverstein RL, Hajjar DP, Cohen PA, Frazier WA, Hoff HF, Hazen SL. Macrophage scavenger receptor CD36 is the major receptor for LDL modified by monocyte-generated reactive nitrogen species. The Journal of clinical investigation. 2000; 105:1095–108. [PubMed: 10772654]
10. Nabel EG, Braunwald E. A tale of coronary artery disease and myocardial infarction. The New England journal of medicine. 2012; 366:54–63. [PubMed: 22216842]
11. Mozaffarian D, Benjamin EJ, Go AS, Arnett DK, Blaha MJ, Cushman M, de Ferranti S, Despres JP, Fullerton HJ, Howard VJ, Huffman MD, Judd SE, Kissela BM, Lackland DT, Lichtman JH, Lisabeth LD, Liu S, Mackey RH, Matchar DB, McGuire DK, Mohler ER 3rd, Moy CS, Muntner P, Mussolino ME, Nasir K, Neumar RW, Nichol G, Palaniappan L, Pandey DK, Reeves MJ, Rodriguez CJ, Sorlie PD, Stein J, Towfighi A, Turan TN, Virani SS, Willey JZ, Woo D, Yeh RW, Turner MB. American Heart Association Statistics, C., Stroke Statistics, S. Heart disease and stroke statistics--2015 update: a report from the American Heart Association. Circulation. 2015; 131:e29–322. [PubMed: 25520374]
12. WHO. Cardiovascular Diseases (CVDs). World Health Organization; 2016.
13. Field JM, Hazinski MF, Sayre MR, Chameides L, Schexnayder SM, Hemphill R, Samson RA, Kattwinkel J, Berg RA, Bhanji F, Cave DM, Jauch EC, Kudenchuk PJ, Neumar RW, Peberdy MA, Perlman JM, Sinz E, Travers AH, Berg MD, Billi JE, Eigel B, Hickey RW, Kleinman ME, Link MS, Morrison LJ, O'Connor RE, Shuster M, Callaway CW, Cucchiara B, Ferguson JD, Rea TD, Vanden Hoek TL. Part 1: executive summary: 2010 American Heart Association Guidelines for Cardiopulmonary Resuscitation and Emergency Cardiovascular Care. Circulation. 2010; 122:S640–56. [PubMed: 20956217]
14. Townsend N, Nichols M, Scarborough P, Rayner M. Cardiovascular disease in Europe--epidemiological update 2015. European heart journal. 2015; 36:2696–705. [PubMed: 26306399]
15. Ross R. Atherosclerosis--an inflammatory disease. N Engl J Med. 1999; 340:115–26. [PubMed: 9887164]
16. Park YM, Febbraio M, Silverstein RL. CD36 modulates migration of mouse and human macrophages in response to oxidized LDL and may contribute to macrophage trapping in the arterial intima. The Journal of clinical investigation. 2009; 119:136–45. [PubMed: 19065049]
17. Mahankali M, Henkels KM, Speranza F, Gomez-Cambronero J. A non-mitotic role for Aurora kinase A as a direct activator of cell migration upon interaction with PLD, FAK and Src. J Cell Sci. 2015; 128:516–26. [PubMed: 25501815]
18. Tang H, Li A, Bi J, Veltman DM, Zech T, Spence HJ, Yu X, Timpson P, Insall RH, Frame MC, Machesky LM. Loss of Scar/WAVE complex promotes N-WASP- and FAK-dependent invasion. Curr Biol. 2013; 23:107–17. [PubMed: 23273897]
19. Serrels B, Serrels A, Brunton VG, Holt M, McLean GW, Gray CH, Jones GE, Frame MC. Focal adhesion kinase controls actin assembly via a FERM-mediated interaction with the Arp2/3 complex. Nat Cell Biol. 2007; 9:1046–56. [PubMed: 17721515]
20. Murphy DA, Courtneidge SA. The 'ins' and 'outs' of podosomes and invadopodia: characteristics, formation and function. Nat Rev Mol Cell Biol. 2011; 12:413–26. [PubMed: 21697900]
21. Schober A, Siess W. Lysophosphatidic acid in atherosclerotic diseases. Br J Pharmacol. 2012; 167:465–82. [PubMed: 22568609]
22. Eleniste PP, Bruzzaniti A. Focal adhesion kinases in adhesion structures and disease. Journal of signal transduction. 2012; 2012:296450. [PubMed: 22888421]
23. Gomez-Cambronero J. New concepts in phospholipase D signaling in inflammation and cancer. Scientific World Journal. 2010; 10:1356–69. [PubMed: 20623096]
24. McDermott M, Wakelam MJO, Morris AJ. Phospholipase D. Biochemistry and cell biology = Biochimie et biologie cellulaire. 2004; 82:225–53. [PubMed: 15052340]
25. Frohman MA. The phospholipase D superfamily as therapeutic targets. Trends in pharmacological sciences. 2015; 36:137–44. [PubMed: 25661257]
26. Bruntz RC, Lindsley CW, Brown HA. Phospholipase D signaling pathways and phosphatidic acid as therapeutic targets in cancer. Pharmacological reviews. 2014; 66:1033–79. [PubMed: 25244928]

27. Gomez-Cambronero J, Kantonen S. A river runs through it: how autophagy, senescence, and phagocytosis could be linked to phospholipase D by Wnt signaling. J Leukoc Biol. 2014; 96:779–84. [PubMed: 25082152]
28. Stegner D, Thielmann I, Kraft P, Frohman MA, Stoll G, Nieswandt B. Pharmacological inhibition of phospholipase D protects mice from occlusive thrombus formation and ischemic stroke--brief report. Arterioscler Thromb Vasc Biol. 2013; 33:2212–7. [PubMed: 23868933]
29. Olala LO, Seremwe M, Tsai YY, Bollag WB. A role for phospholipase D in angiotensin II-induced protein kinase D activation in adrenal glomerulosa cell models. Mol Cell Endocrinol. 2013; 366:31–7. [PubMed: 23178798]
30. Thielmann I, Stegner D, Kraft P, Hagedorn I, Krohne G, Kleinschnitz C, Stoll G, Nieswandt B. Redundant functions of phospholipases D1 and D2 in platelet alpha-granule release. Journal of thrombosis and haemostasis : JTH. 2012; 10:2361–72. [PubMed: 22974101]
31. Noh JY, Lim KM, Bae ON, Chung SM, Lee SW, Joo KM, Lee SD, Chung JH. Procoagulant and prothrombotic activation of human erythrocytes by phosphatidic acid. Am J Physiol Heart Circ Physiol. 2010; 299:H347–55. [PubMed: 20495145]
32. Elvers M, Stegner D, Hagedorn I, Kleinschnitz C, Braun A, Kuijpers ME, Boesl M, Chen Q, Heemskerk JW, Stoll G, Frohman MA, Nieswandt B. Impaired alpha(IIb)beta(3) integrin activation and shear-dependent thrombus formation in mice lacking phospholipase D1. Sci Signal. 2010; 3:ra1. [PubMed: 20051593]
33. Kim AS, Kakalis LT, Abdul-Manan N, Liu GA, Rosen MK. Autoinhibition and activation mechanisms of the Wiskott-Aldrich syndrome protein. Nature. 2000; 404:151–8. [PubMed: 10724160]
34. Marchand JB, Kaiser DA, Pollard TD, Higgs HN. Interaction of WASP/Scar proteins with actin and vertebrate Arp2/3 complex. Nat Cell Biol. 2001; 3:76–82. [PubMed: 11146629]
35. Panchal SC, Kaiser DA, Torres E, Pollard TD, Rosen MK. A conserved amphipathic helix in WASP/Scar proteins is essential for activation of Arp2/3 complex. Nat Struct Biol. 2003; 10:591–8. [PubMed: 12872157]
36. Rohatgi R, Ho HY, Kirschner MW. Mechanism of N-WASP activation by CDC42 and phosphatidylinositol 4,5-bisphosphate. J Cell Biol. 2000; 150:1299–310. [PubMed: 10995436]
37. Thrasher AJ. WASp in immune-system organization and function. Nat Rev Immunol. 2002; 2:635–46. [PubMed: 12209132]
38. Thrasher AJ, Burns S, Lorenzi R, Jones GE. The Wiskott-Aldrich syndrome: disordered actin dynamics in haematopoietic cells. Immunol Rev. 2000; 178:118–28. [PubMed: 11213796]
39. Tomasevic N, Jia Z, Russell A, Fujii T, Hartman JJ, Clancy S, Wang M, Beraud C, Wood KW, Sakowicz R. Differential regulation of WASP and N-WASP by Cdc42, Rac1, Nck, and PI(4,5)P2. Biochemistry. 2007; 46:3494–502. [PubMed: 17302440]
40. Kantonen S, Hatton N, Mahankali M, Henkels KM, Park H, Cox D, Gomez-Cambronero J. A novel phospholipase D2-Grb2-WASp heterotrimer regulates leukocyte phagocytosis in a two-step mechanism. Mol Cell Biol. 2011; 31:4524–37. [PubMed: 21930784]
41. Henkels KM, Boivin GP, Dudley ES, Berberich SJ, Gomez-Cambronero J. Phospholipase D (PLD) drives cell invasion, tumor growth and metastasis in a human breast cancer xenograph model. Oncogene. 2013; 32:5551–62. [PubMed: 23752189]
42. Chen Q, Hongu T, Sato T, Zhang Y, Ali W, Cavallo J-A, van der Velden A, Tian H, Di Paolo G, Nieswandt B, Kanaho Y, Frohman MA. Key roles for the lipid signaling enzyme phospholipase d1 in the tumor microenvironment during tumor angiogenesis and metastasis. Science signaling. 2012; 5:ra79. [PubMed: 23131846]
43. Oliveira TG, Chan RB, Tian H, Laredo M, Shui G, Staniszewski A, Zhang H, Wang L, Kim T-W, Duff KE, Wenk MR, Arancio O, Di Paolo G. Phospholipase d2 ablation ameliorates Alzheimer's disease-linked synaptic dysfunction and cognitive deficits. The Journal of neuroscience : the official journal of the Society for Neuroscience. 2010; 30:16419–28. [PubMed: 21147981]
44. Swamydas M, Lionakis MS. Isolation, purification and labeling of mouse bone marrow neutrophils for functional studies and adoptive transfer experiments. Journal of visualized experiments : JoVE. 2013:e50586. [PubMed: 23892876]

45. Steinbrecher UP, Parthasarathy S, Leake DS, Witztum JL, Steinberg D. Modification of low density lipoprotein by endothelial cells involves lipid peroxidation and degradation of low density lipoprotein phospholipids. Proc Natl Acad Sci U S A. 1984; 81:3883–7. [PubMed: 6587396]
46. Steinbrecher UP, Witztum JL, Parthasarathy S, Steinberg D. Decrease in reactive amino groups during oxidation or endothelial cell modification of LDL. Correlation with changes in receptor-mediated catabolism. Arteriosclerosis. 1987; 7:135–43. [PubMed: 3107534]
47. Steinberg D, Parthasarathy S, Carew TE, Khoo JC, Witztum JL. Beyond cholesterol. Modifications of low-density lipoprotein that increase its atherogenicity. N Engl J Med. 1989; 320:915–24. [PubMed: 2648148]
48. Lu M, Gursky O. Aggregation and fusion of low-density lipoproteins in vivo and in vitro. Biomol Concepts. 2013; 4:501–18. [PubMed: 25197325]
49. Oorni K, Pentikainen MO, Ala-Korpela M, Kovanen PT. Aggregation, fusion, and vesicle formation of modified low density lipoprotein particles: molecular mechanisms and effects on matrix interactions. J Lipid Res. 2000; 41:1703–14. [PubMed: 11060340]
50. Lougheed M, Steinbrecher UP. Mechanism of uptake of copper-oxidized low density lipoprotein in macrophages is dependent on its extent of oxidation. J Biol Chem. 1996; 271:11798–805. [PubMed: 8662601]
51. Khoo JC, Miller E, McLoughlin P, Steinberg D. Prevention of low density lipoprotein aggregation by high density lipoprotein or apolipoprotein A-I. J Lipid Res. 1990; 31:645–52. [PubMed: 2112580]
52. Manzanero S. Generation of mouse bone marrow-derived macrophages. Methods Mol Biol. 2012; 844:177–81. [PubMed: 22262442]
53. Deutsch MJ, Schriever SC, Roscher AA, Ensenauer R. Digital image analysis approach for lipid droplet size quantitation of Oil Red O-stained cultured cells. Anal Biochem. 2014; 445:87–9. [PubMed: 24120410]
54. Glass AM, Wolf BJ, Schneider KM, Princiotta MF, Taffet SM. Connexin43 is dispensable for phagocytosis. J Immunol. 2013; 190:4830–5. [PubMed: 23554311]
55. Reichard AC, Cheemarla NR, Bigley NJ. SOCS1/3 expression levels in HSV-1-infected, cytokine-polarized and -unpolarized macrophages. J Interferon Cytokine Res. 2015; 35:32–41. [PubMed: 24956148]
56. Dunn KW, Kamocka MM, McDonald JH. A practical guide to evaluating colocalization in biological microscopy. Am J Physiol Cell Physiol. 2011; 300:C723–42. [PubMed: 21209361]
57. Adler J, Parmryd I. Quantifying colocalization by correlation: the Pearson correlation coefficient is superior to the Mander's overlap coefficient. Cytometry A. 2010; 77:733–42. [PubMed: 20653013]
58. Ayari H, Bricca G. Identification of two genes potentially associated in iron-heme homeostasis in human carotid plaque using microarray analysis. J Biosci. 2013; 38:311–5. [PubMed: 23660665]
59. Ganesan R, Mahankali M, Alter G, Gomez-Cambronero J. Two sites of action for PLD2 inhibitors: The enzyme catalytic center and an allosteric, phosphoinositide biding pocket. Biochim Biophys Acta. 2015; 1851:261–72. [PubMed: 25532944]
60. Su W, Yeku O, Olepu S, Genna A, Park J-S, Ren H, Du G, Gelb MH, Morris AJ, Frohman MA. 5-Fluoro-2-indolyl des-chlorohalopemide (FIPI), a phospholipase D pharmacological inhibitor that alters cell spreading and inhibits chemotaxis. Molecular pharmacology. 2009; 75:437–46. [PubMed: 19064628]
61. Ali WH, Chen Q, Delgiorno KE, Su W, Hall JC, Hongu T, Tian H, Kanaho Y, Di Paolo G, Crawford HC, Frohman MA. Deficiencies of the lipid-signaling enzymes phospholipase D1 and D2 alter cytoskeletal organization, macrophage phagocytosis, and cytokine-stimulated neutrophil recruitment. PloS one. 2013; 8:e55325. [PubMed: 23383154]
62. Corrotte M, Chasserot-Golaz S, Huang P, Du G, Ktistakis NT, Frohman MA, Vitale N, Bader M-F, Grant NJ. Dynamics and function of phospholipase D and phosphatidic acid during phagocytosis. Traffic (Copenhagen, Denmark). 2006; 7:365–77.
63. Relevy NZ, Bechor S, Harari A, Ben-Amotz A, Kamari Y, Harats D, Shaish A. The Inhibition of Macrophage Foam Cell Formation by 9-Cis beta-Carotene Is Driven by BCMO1 Activity. Plos One. 2015; 10

64. Wu C, Chen R, Liu M, Liu D, Li X, Wang S, Niu S, Guo P, Lin W. Spiromastixones Inhibit Foam Cell Formation via Regulation of Cholesterol Efflux and Uptake in RAW264.7 Macrophages. Mar Drugs. 2015; 13:6352–65. [PubMed: 26473890]

65. Xu S, Huang Y, Xie Y, Lan T, Le K, Chen J, Chen S, Gao S, Xu X, Shen X, Huang H, Liu P. Evaluation of foam cell formation in cultured macrophages: an improved method with Oil Red O staining and DiI-oxLDL uptake. Cytotechnology. 2010; 62:473–81. [PubMed: 21076992]

66. Du G, Huang P, Liang BT, Frohman MA. Phospholipase D2 localizes to the plasma membrane and regulates angiotensin II receptor endocytosis. Mol Biol Cell. 2004; 15:1024–30. [PubMed: 14718562]

67. Freyberg Z, Sweeney D, Siddhanta A, Bourgoin S, Frohman M, Shields D. Intracellular localization of phospholipase D1 in mammalian cells. Mol Biol Cell. 2001; 12:943–55. [PubMed: 11294898]

68. Lee JS, Kim IS, Kim JH, Cho W, Suh PG, Ryu SH. Determination of EGFR endocytosis kinetic by auto-regulatory association of PLD1 with mu2. PLoS One. 2009; 4:e7090. [PubMed: 19763255]

69. Scott SA, Selvy PE, Buck JR, Cho HP, Criswell TL, Thomas AL, Armstrong MD, Arteaga CL, Lindsley CW, Brown HA. Design of isoform-selective phospholipase D inhibitors that modulate cancer cell invasiveness. Nat Chem Biol. 2009; 5:108–17. [PubMed: 19136975]

70. Collot-Teixeira S, Martin J, McDermott-Roe C, Poston R, McGregor JL. CD36 and macrophages in atherosclerosis. Cardiovasc Res. 2007; 75:468–77. [PubMed: 17442283]

71. Montano EN, Boullier A, Almazan F, Binder CJ, Witztum JL, Hartvigsen K. Development and application of a nonradioactive binding assay of oxidized low-density lipoprotein to macrophage scavenger receptors. J Lipid Res. 2013; 54:3206–14. [PubMed: 23997238]

72. Yu XH, Fu YC, Zhang DW, Yin K, Tang CK. Foam cells in atherosclerosis. Clin Chim Acta. 2013; 424:245–52. [PubMed: 23782937]

73. Rahaman SO, Lennon DJ, Febbraio M, Podrez EA, Hazen SL, Silverstein RL. A CD36-dependent signaling cascade is necessary for macrophage foam cell formation. Cell Metab. 2006; 4:211–21. [PubMed: 16950138]

74. Silverstein RL, Li W, Park YM, Rahaman SO. Mechanisms of cell signaling by the scavenger receptor CD36: implications in atherosclerosis and thrombosis. Trans Am Clin Climatol Assoc. 2010; 121:206–20. [PubMed: 20697562]

75. Jiang H, Lu Z, Luo JQ, Wolfman A, Foster DA. Ras mediates the activation of phospholipase D by v-Src. J Biol Chem. 1995; 270:6006–9. [PubMed: 7890731]

76. Frondorf K, Henkels KM, Frohman MA, Gomez-Cambronero J. Phosphatidic acid (PA) is a leukocyte chemoattractant that acts through S6 kinase signaling. J Biol Chem. 2010; 285:15837–15847. [PubMed: 20304930]

77. Lehman N, Di Fulvio M, McCray N, Campos I, Tabatabaian F, Gomez-Cambronero J. Phagocyte cell migration is mediated by phospholipases PLD1 and PLD2. Blood. 2006; 108:3564–72. [PubMed: 16873675]

78. Kassas N, Tanguy E, Thahouly T, Fouillen L, Heintz D, Chasserot-Golaz S, Bader M-F, Grant NJ, Vitale N. Comparative Characterization of Phosphatidic Acid Sensors and Their Localization during Frustrated Phagocytosis. The Journal of biological chemistry. 2017; 292:4266–4279. [PubMed: 28115519]

79. Henkels KM, Muppani NR, Gomez-Cambronero J. PLD-Specific Small-Molecule Inhibitors Decrease Tumor-Associated Macrophages and Neutrophils Infiltration in Breast Tumors and Lung and Liver Metastases. PLoS One. 2016; 11:e0166553. [PubMed: 27851813]

80. Miller TE, Gomez-Cambronero J. A feedback mechanism between PLD and deadenylase PARN for the shortening of eukaryotic poly(A) mRNA tails that is deregulated in cancer cells. Biology open. 2017; 6:176–186. [PubMed: 28011629]

81. Iyer SS, Barton JA, Bourgoin S, Kusner DJ. Phospholipases D1 and D2 coordinately regulate macrophage phagocytosis. J Immunol. 2004; 173:2615–23. [PubMed: 15294978]

82. Finn AV, Nakano M, Narula J, Kolodgie FD, Virmani R. Concept of Vulnerable/Unstable Plaque. Arteriosclerosis Thrombosis and Vascular Biology. 2010; 30:1282–1292.

83. Schwartz CJ, Valente AJ, Sprague EA, Kelley JL, Cayatte AJ, Mowery J. Atherosclerosis - Potential Targets for Stabilization and Regression. Circulation. 1992; 86:117–123.

84. Barbieri SS, Cavalca V, Eligini S, Brambilla M, Caiani A, Tremoli E, Colli S. Apocynin prevents cyclooxygenase 2 expression in human monocytes through NADPH oxidase and glutathione redox-dependent mechanisms. Free radical biology & medicine. 2004; 37:156–65. [PubMed: 15203187]

85. Hansson GK, Robertson AK, Soderberg-Naucler C. Inflammation and atherosclerosis. Annual review of pathology. 2006; 1:297–329.

86. Mietus-Snyder M, Friera A, Glass CK, Pitas RE. Regulation of scavenger receptor expression in smooth muscle cells by protein kinase C: a role for oxidative stress. Arteriosclerosis, thrombosis, and vascular biology. 1997; 17:969–78.

87. Lee HK, Yeo S, Kim JS, Lee JG, Bae YS, Lee C, Baek SH. Protein kinase C-eta and phospholipase D2 pathway regulates foam cell formation via regulator of G protein signaling 2. Mol Pharmacol. 2010; 78:478–85. [PubMed: 20558593]

88. Koch T, Wu DF, Yang LQ, Brandenburg LO, Hollt V. Role of phospholipase D2 in the agonist-induced and constitutive endocytosis of G-protein coupled receptors. J Neurochem. 2006; 97:365–72. [PubMed: 16539674]

89. Mahankali M, Peng HJ, Cox D, Gomez-Cambronero J. The mechanism of cell membrane ruffling relies on a phospholipase D2 (PLD2), Grb2 and Rac2 association. Cell Signal. 2011; 23:1291–8. [PubMed: 21419846]

90. Schonberger T, Jurgens T, Muller J, Armbruster N, Niermann C, Gorressen S, Sommer J, Tian H, di Paolo G, Scheller J, Fischer JW, Gawaz M, Elvers M. Pivotal role of phospholipase D1 in tumor necrosis factor-alpha-mediated inflammation and scar formation after myocardial ischemia and reperfusion in mice. Am J Pathol. 2014; 184:2450–64. [PubMed: 25046692]

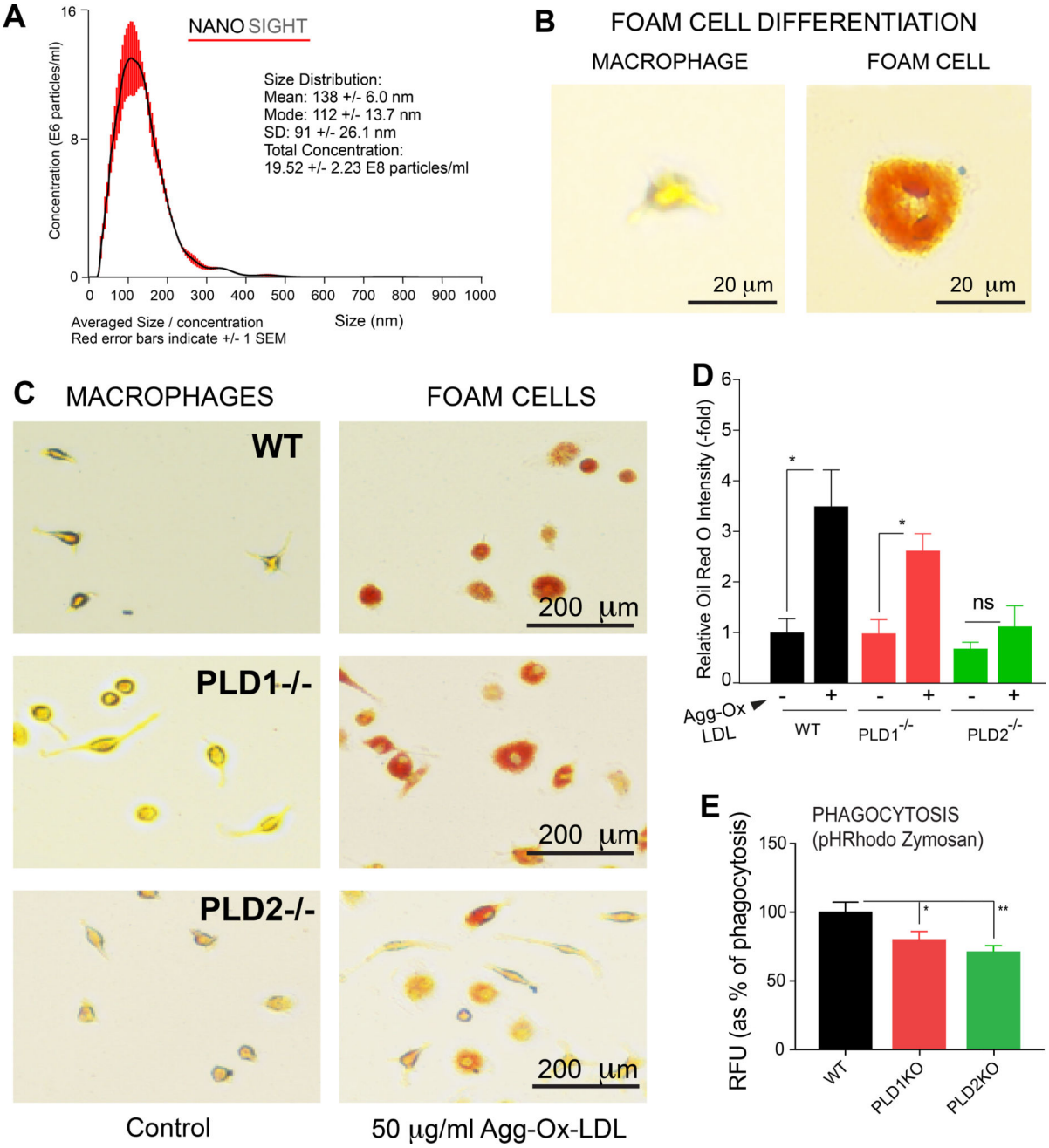

Figure 1. Macrophage phagocytosis of oxidized LDL is PLD2-dependent

(**A**) Agg-Ox-LDL particles were prepared as described in Methods. Their physical properties were measured in a NanoSight NS300 with a 405 nm laser instrument (Malvern Instruments, United Kingdom). Shown is a typical example. (**B**) Photomicrographs of representative Oil Red O-stained macrophages versus Agg-Ox-LDL-laden foam cells. Scale bar = 20 μm. (**C**) Representative fields of view from photomicrographs of untreated and Agg-Ox-LDL -treated (50 μg/ml) BMDM from WT and PLD knockout mice. Phagocytosis of Agg-Ox-LDL by BMDM was performed in biological triplicates and technical duplicates, with sample size n~120 cells read for each condition. Scale bar = 200 μm. (**C**)

Quantification of the relative densities of Oil Red O staining from foam cells from panels similar to those shown in (**D**) in terms of the mean density (-fold) ± SEM with experimental conditions indicated in (C). (**E**) Phagocytosis of phRhodo (red) Zymosan beads by BMDM. Phagocytosis of Zymosan was performed in biological triplicates and technical duplicates, with sample size n~1×10^5 cells/well with zymosan 1:50 for each condition.

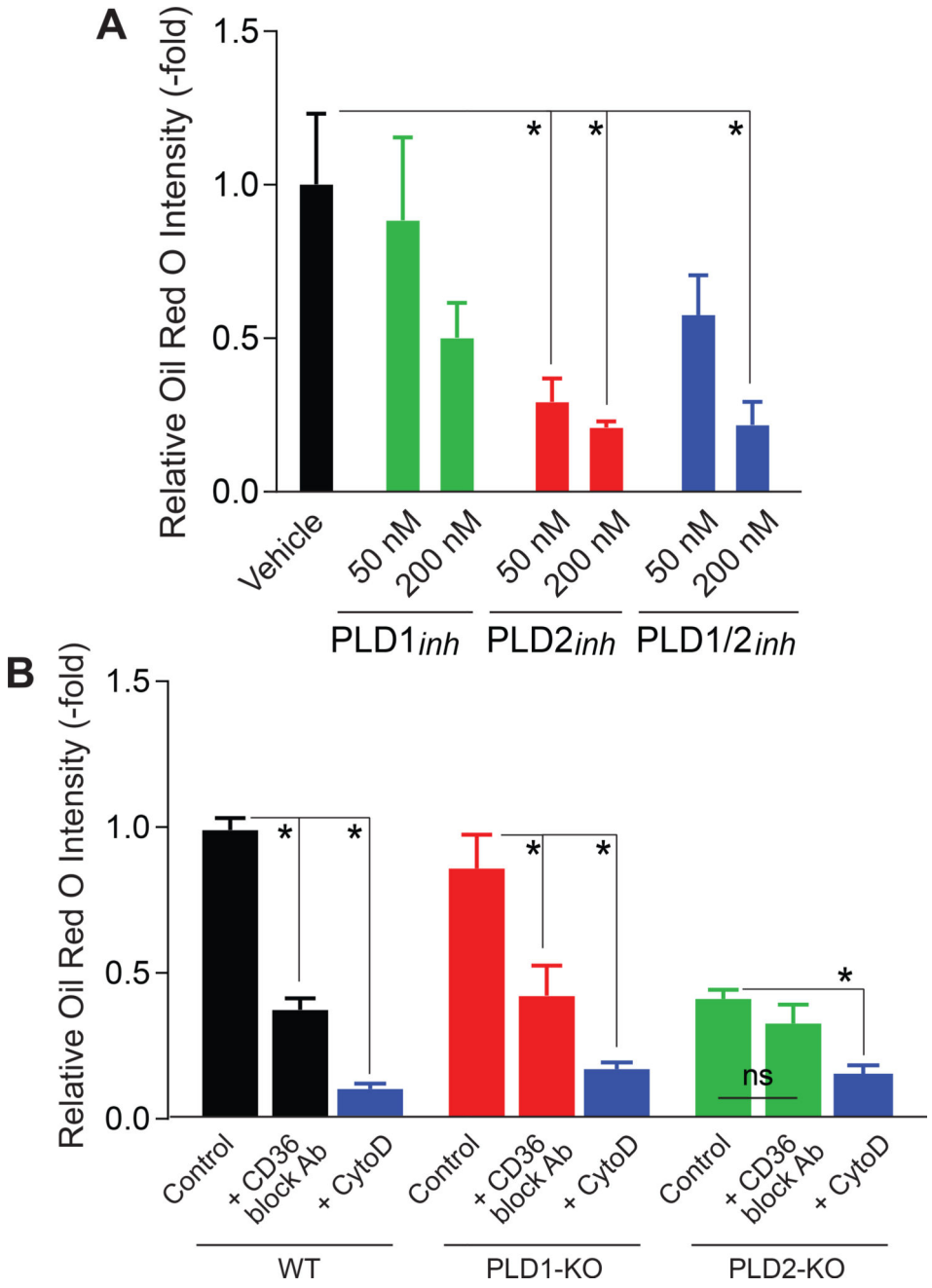

Figure 2. Inhibition of PLD reduces Agg-Ox-LDL phagocytosis

(**A**) BMDM from WT mice were used for foam cell phagocytosis assays of Agg-Ox-LDL in the presence of 50 nM or 200 nM PLD-specific inhibitors: a PLD1-selective NBOD (VU10155069), a PLD2-selective NFOT (VU0364739) and a dual PLD1/2 inhibitor (FIPI). Results are expressed in terms of relative Oil red-O intensity compared to vehicle treated samples in a bar graph. Phagocytosis of Agg-Ox-LDL with PLD inhibitors was performed in biological triplicates and technical duplicates, with sample size n~100 cells read for each condition. (**B**) BMDM from WT, PLD1 KO and PLD2 KO mice were differentiated into macrophages, blocked with anti-CD36 antibody or with 10 μM cytochalasin D, prior to foam

cell formation assay with Agg-Ox-LDL. All experiments were in 3 biological replicates and 2 technical replicates. The symbols * denote statistically significant ($p<0.05$) changes between samples and controls.

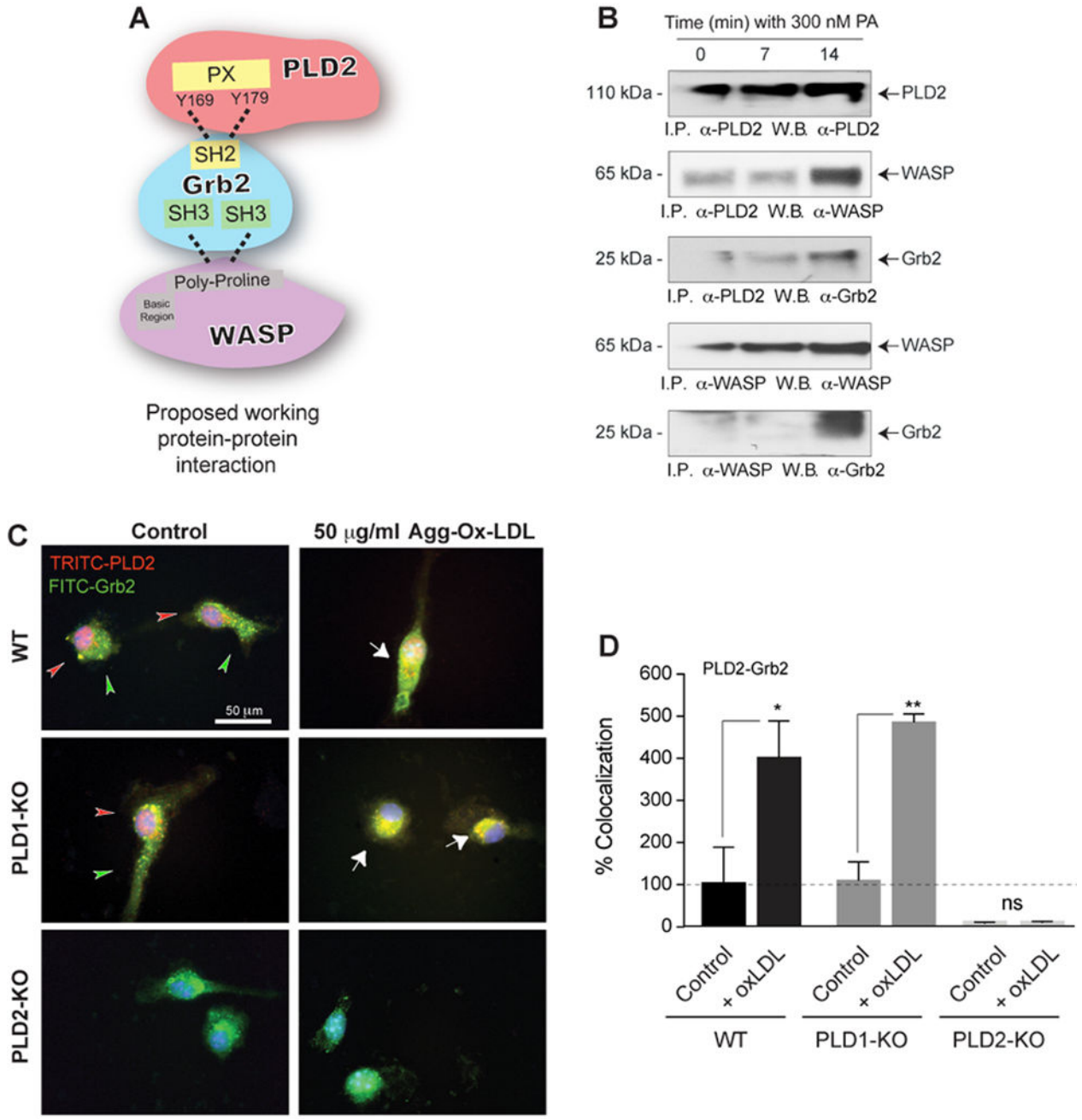

Figure 3. PLD2 colocalizes with adaptor protein Grb2 during foam cell formation

(**A**) Schematic of the interaction sites between PLD2, Growth factor receptor-bound protein 2 (Grb2) and actin-polymerizing Wiskott-Aldrich syndrome protein (WASP). (**B**) Macrophages were treated with 300 nM phosphatidic acid (dioleoyl-PA) for 0, 7 or 14 min. Cell lysates were immunoprecipitated using Protein-G agarose linked to antibodies specific for PLD2, WASP or Grb2 and used for SDS-PAGE. Detection of the protein-protein interactions on subsequent Western blots using a two protein approach indicates protein-protein interaction occurred between PLD2 and WASP, between PLD2 and Grb2 and between WASP and Grb2, which suggests formation of a protein heterotrimeric complex

(PLD2-Grb2-WASp) in the presence of PA (i.e., in conditions where PLD2 would be activated). (**C**) BMDMs with or without 50 μg/ml oxLDL treatment were subject to immuno-staining with TRITC-PLD2 and FITC-Grb2. Scale bar = 50 μm. Red and green arrowheads point at regions where staining is separated whereas white arrows point at areas where there is signal co-localization. (**D**) Co-localization was quantified using ImageJ software with ~2–4 cells per field; 6 fields; n=3 independent experiments, by determining the Pearson's coefficient, which was then plotted as % of co-localization (yellow=TRITC-PLD2 and FITC-Grb2).

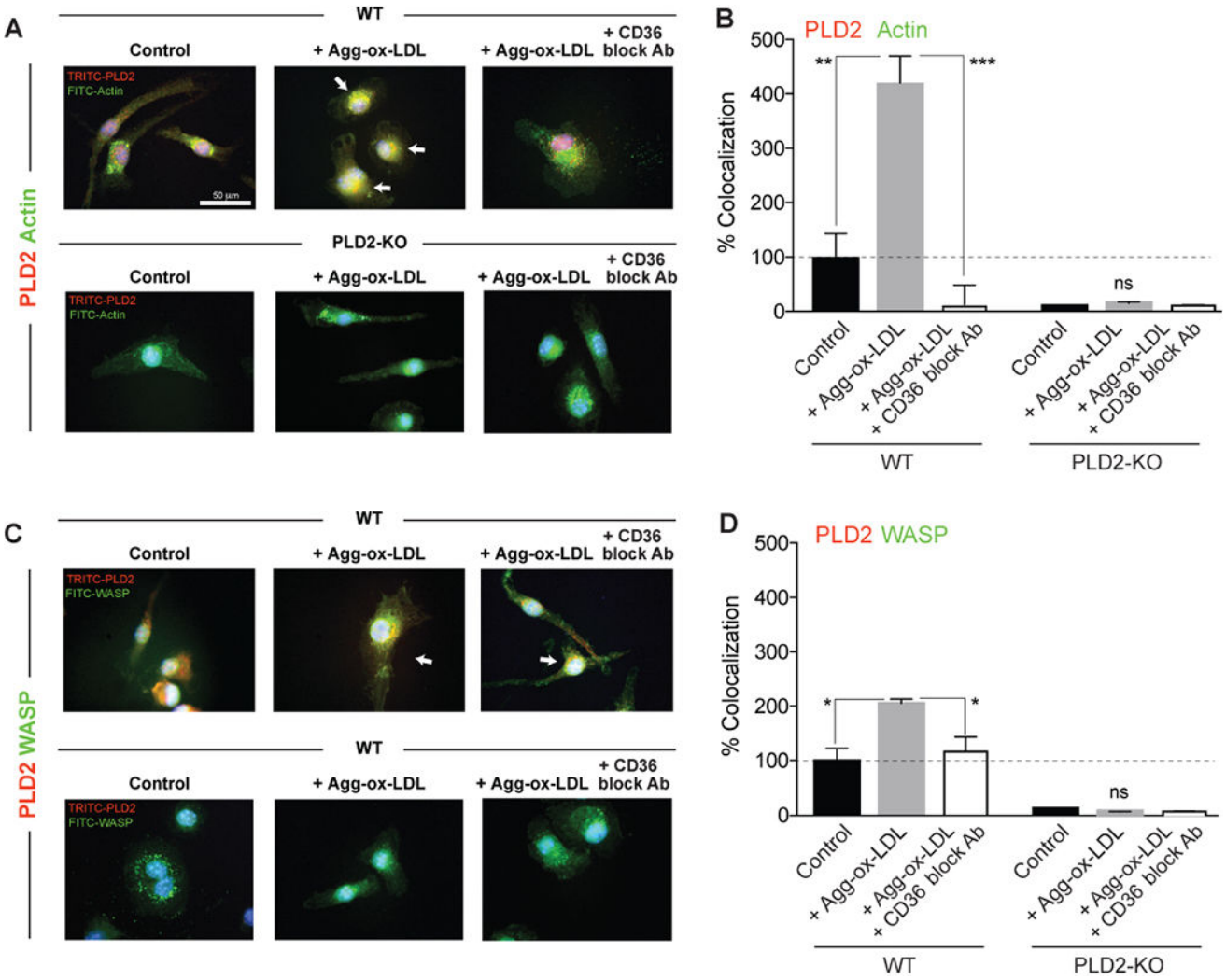

Figure 4. Wiskott-Aldrich syndrome protein (WASP) and Actin colocalize with PLD2 at the time of ox-LDL phagocytosis

BMDMs from WT or PLD2-KO mice were untreated or treated with 50 μg/ml Agg-Ox-LDL in the absence or presence of anti-CD36 blocking monoclonal antibody followed by immuno-staining with TRITC-PLD2/FITC-actin (**A,B**), or TRITC-PLD2/FITC-WASP (**C,D**). Arrows pointing at yellow fluorescence indicate co-localization. Scale bar = 50 μm. Quantification of co-localization for PLD2-Actin **(B)** or PLD2-WASP **(D)** was done using ImageJ software with ~2–4 cells per field; 6 fields; n=3 independent experiments, by determining the Pearson's coefficient, which was then plotted as % of co-localization (yellow=TRITC-PLD2 and FITC-Actin or TRITC-PLD2 FITC-WASP).

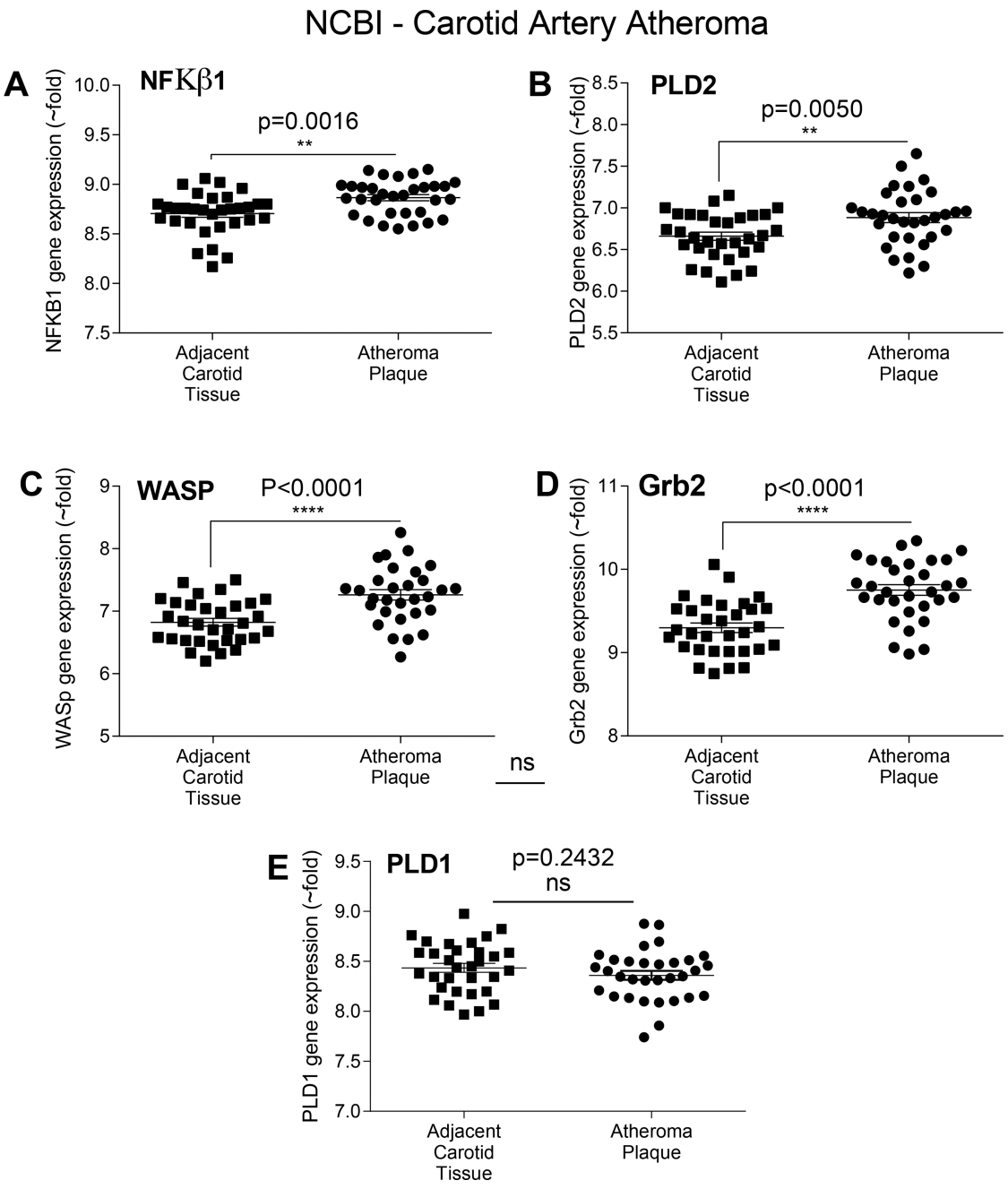

Figure 5. Bioinformatic analysis of PLD and its signaling proteins in human atheroma plaque tissues

Microarray data were from the NCBI Gene Expression Omnibus (GEO) and specifically from the carotid artery atheroma dataset [58]. (**A–E**) NFκβ (p=0.0016) (used here as a proxis for inflammation), PLD2 (p=0.005), Grb2 (p<0.0001) and WASP (p<0.0001) are significantly upregulated in diseased atheroma plaques, while PLD1 is not (p=0.2432). The symbols * denote statistically significant (p<0.05) increases between atheroma plaque and control adjacent carotid artery samples.

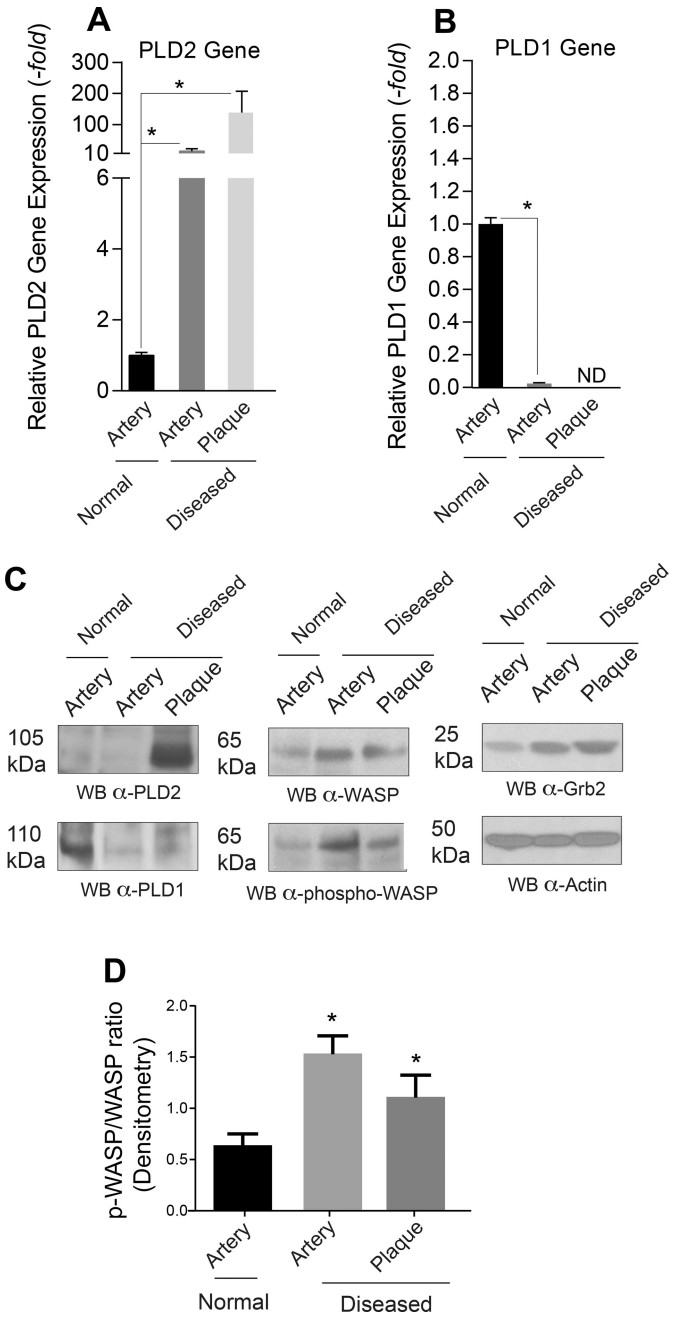

Figure 6. PLD2, Grb2 and phospho-WASP are upregulated in diseased artery tissues

Human patient samples comprised of normal, non-diseased popliteal artery and diseased popliteal artery and the atheromatous plaque contained within it were used for qRT-PCR and SDS-PAGE/western blot analyses. (**A–B**) Relative mRNA expression levels of PLD2 (**A**), PLD1 (**B**), expressed in terms of mean (-fold) expression ± SEM relative to housekeeping gene (TATA Binding Protein, TBP). (**C**) Protein expression levels of PLD2 and Actin, PLD1, WASP and phospho-WASP and Grb2. Actin is the equal protein loading control. The Western blots and gene expression assays were done in biological triplicates (n=3). (**D**) Densitometry ratio of p-WASP/WASP shown in bar graph. The symbols * denote

statistically significant ($p<0.05$) changes, respectively, between samples and controls using one-way ANOVA or t-test.

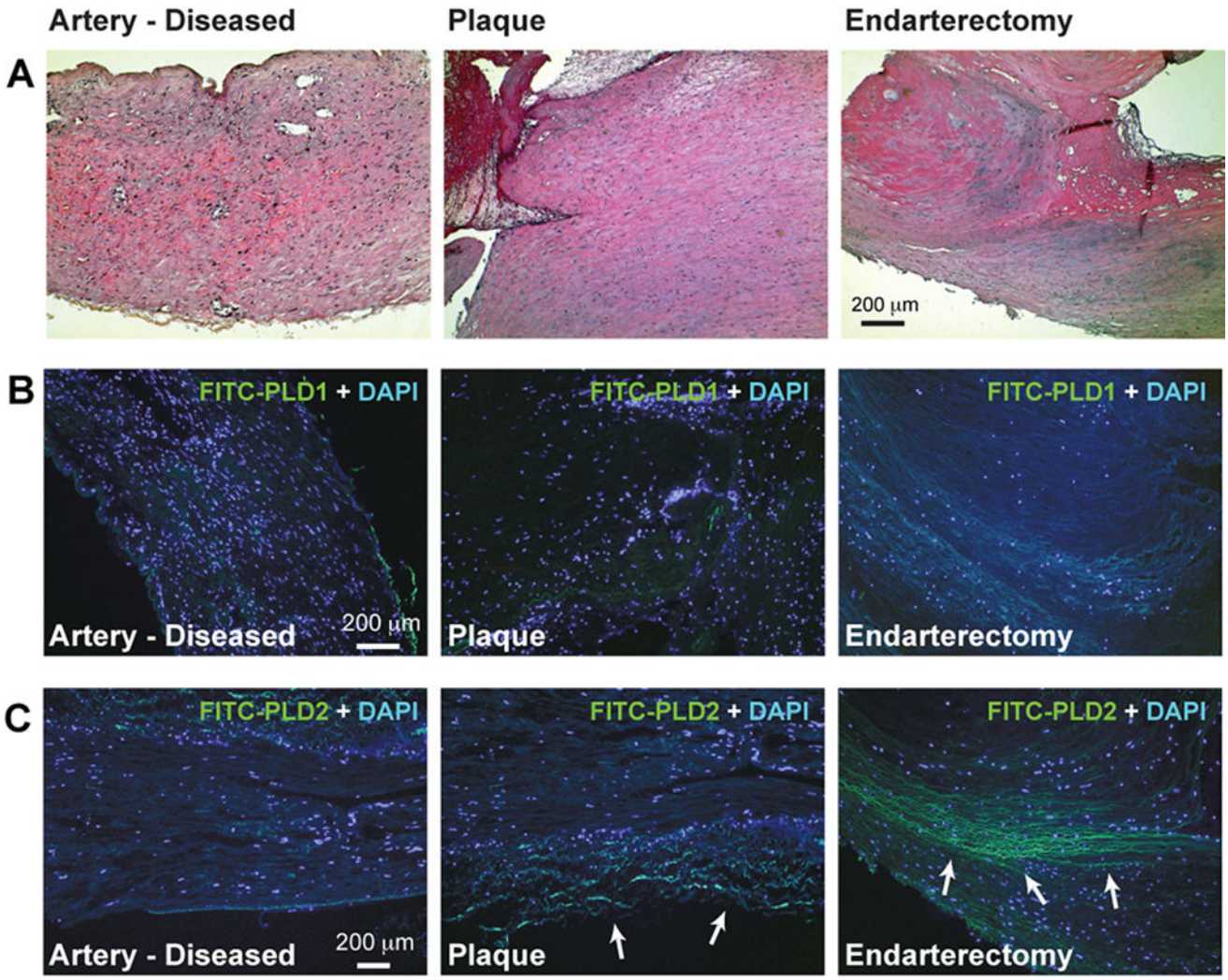

Figure 7. PLD2, WASP and Grb2 are overexpressed in diseased human artery samples

Diseased human arteries, plaque from that diseased arteries and plaque removed during endarterectomy samples, which are companions to those shown in the previous figure; they were fixed in paraformaldehyde, paraffin-embedded, sectioned, mounted and used for H&E and immunofluorescence (IF) staining. (**A**) H&E stained samples were magnified at 10×. Scale bar = 200 μm. (**B–C**) IF stained samples for PLD1 (**B**) or PLD2 (**C**). Proteins of interest were FITC stained, while nuclei were stained with DAPI. Merged images of FITC and DAPI staining are shown for each sample. Arrows point at zones were accumulation of PLD2 staining was obvious. IF samples were magnified at 100×. Scale bar = 200 μm.

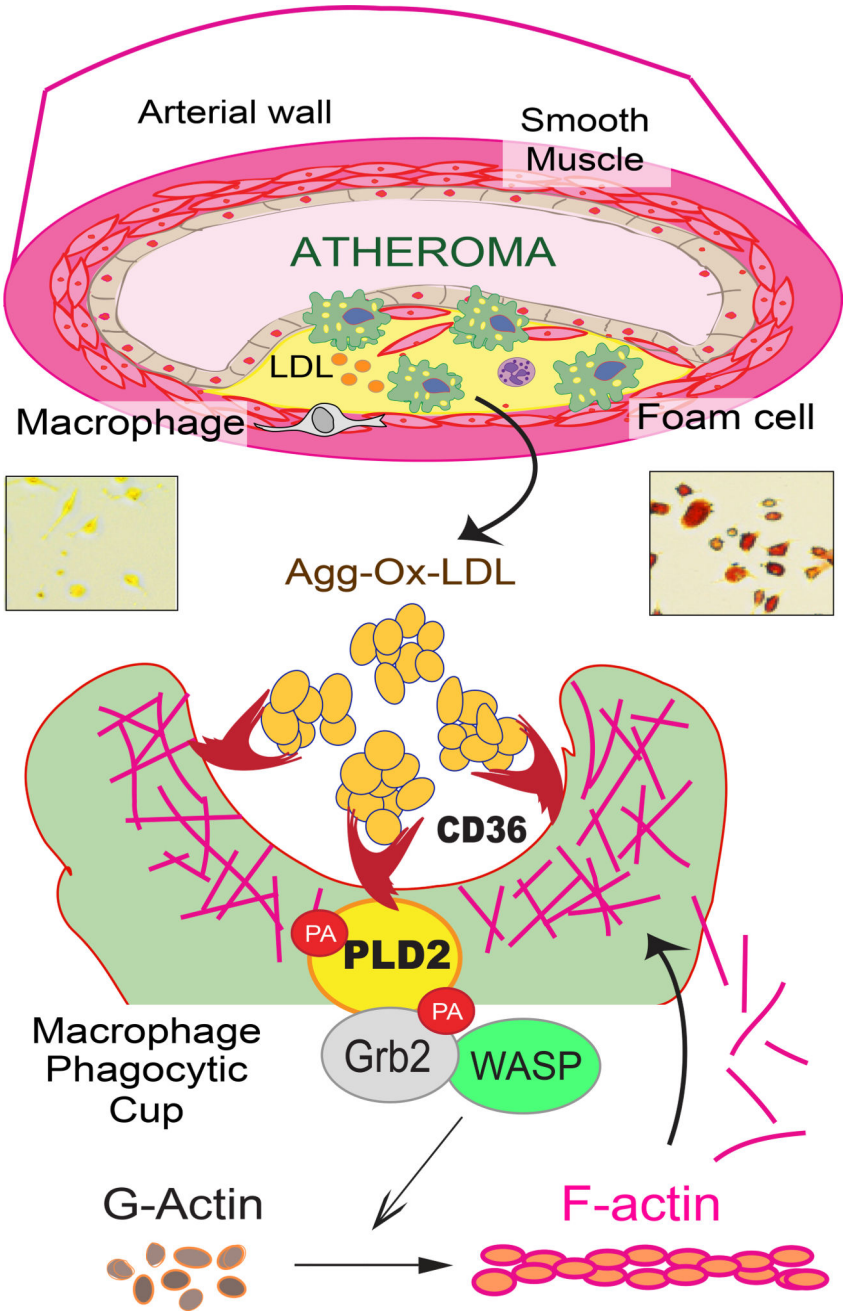

Figure 8. Model of PLD2-mediated foam cell-atherogenesis

Foam cell accumulation leads to atherogenesis. Foam cell formation by Agg-Ox-LDL uptake by scavenger receptor CD36 on macrophages mediates PLD2 interaction with WASP and Grb2 resulting in actin polymerization, that allows phagocytosis as indicated for the first time in this study. See Discussion section for detailed description of the Model.